

# Application of Adaptive Kinetic Modeling for Bias Propagation Reduction in Direct 4D Image Reconstruction

Fotis A. Kotasidis, *Member IEEE*, Julian C. Matthews, *Member IEEE*, Andrew J Reader, *Member IEEE*, Georgios I. Angelis, *Member IEEE*, Habib Zaidi, *Senior Member, IEEE*

**Abstract**— Direct 4D image reconstruction algorithms can improve kinetic parameter precision and accuracy in dynamic PET/CT body imaging but in contrast to post-reconstruction kinetic analysis, errors in badly modeled regions will spatially propagate to regions which are well modeled. To reduce error propagation from erroneous model fits, we propose a new approach to direct 4D image reconstruction by incorporating a newly proposed kinetic modeling strategy. This uses a secondary model to allow a less constrained model fit in regions where an erroneous kinetic model is used and adaptively include a portion of the residuals back into the image, whilst preserving the primary model characteristics in other well modeled regions. Using a digital 4-D phantom to simulate [<sup>15</sup>O]-H<sub>2</sub>O kinetics, we demonstrate substantial bias reduction due to propagation in all kinetic parameters using the proposed 4-D method. Under noisy conditions improvements in bias due to propagation are obtained at the expense of a small increase in bias due to noise and selective inclusion of residuals coming from erroneous kinetic modeling, as opposed to noise, becomes more challenging. However, the overall bias is reduced with improvements depending on the proximity of regions of interest to badly modeled regions and the choice of the secondary model space.

**Index Terms**—Direct 4-D image reconstruction, adaptive kinetic modeling, parametric imaging

## I. INTRODUCTION

DIRECT 4D image reconstruction methods have been shown to improve bias and variance in parameter estimates when applied in neuroreceptor imaging studies [1-3]. However, when applied in the body their behavior becomes complex. Regions with differential delay and dispersion, such as veins carrying the activity from the

injection site and activity delivery through routes other than arterial blood (urinary excretion, liver etc), can be located within the scanned FOV. In such cases, a single model cannot always describe the kinetics within the field of view (FOV) and usually a model which adequately describes the regions of primary interest is selected, with the rest of the regions being badly modeled. This is in contrast to neuroreceptor imaging, where using a single model to describe the underlying temporal distribution of a given tracer is a valid approximation. In our previous work we demonstrated that as opposed to post-reconstruction analysis, where erroneous kinetic modeling results in localized bias in kinetic parameter (which can be excluded from any subsequent analysis), in direct 4D methods, errors from discrepancies between the measured and modeled data during the kinetic modeling step can spatially propagate during the tomographic step [4]. This results in biases propagating from badly modeled regions to regions where the kinetic model accurately describes the underlying kinetics, reducing the benefits of direct 4D methods or even producing more biased kinetic parameter estimates than conventional post reconstruction methods. To avoid bias in erroneously modeled regions from spatially propagating to regions which are of interest, it is critical that the kinetics of all regions in the FOV are accurately described.

In this work, we implement and evaluate a new approach to direct 4D reconstruction. The method is based on the application of a newly proposed kinetic modeling methodology to allow a less constrained fit in regions where the primary model doesn't fit the data, whilst maintaining the primary model in the rest of the regions, in order to reduce kinetic parameter bias propagation [5]. The new direct 4D image reconstruction method is compared with the conventional 4D reconstruction as well as with the post-reconstruction kinetic analysis using noiseless as well as noisy fully 4D simulated data.

## II. THEORY

The method is an extension of a previously proposed 4D EM algorithm for direct kinetic parameter estimation. This algorithm is referred to as the conventional 4D reconstruction method in this work and is based on converting the spatiotemporal 4D maximum likelihood problem, into a tomographic maximum likelihood problem and an image based weighted least squares problem [1]. The algorithm

F. A. Kotasidis is with Division of Nuclear Medicine and Molecular Imaging, Geneva University Hospital, Switzerland and with Wolfson Molecular Imaging Centre, MAHSC, University of Manchester, UK

J.C. Matthews is with the Wolfson Molecular Imaging Centre, MAHSC, University of Manchester, UK

G. I. Angelis is with Brain and Mind Institute, University of Sydney, Australia

A.J. Reader is with Montreal Neurological Institute, McGill University, Canada

Habib Zaidi is with Division of Nuclear Medicine, Geneva University Hospital and Geneva Neuroscience Center, Geneva University, Switzerland

proceeds by alternating between the tomographic EM image update and the pixelwise kinetic modeling steps, using a one-step-late approach to estimate the model weights during the kinetic analysis step.

The new adaptive 4D image reconstruction algorithm introduces an additional step after the primary kinetic modeling step. The method incorporates a new adaptive kinetic modeling framework which uses a secondary more general model to model any structure in the residuals, which can result from the application of an inadequate primary kinetic model [5]. If structured residuals are identified, a portion of these are adaptively included back into the image, in regions for which the primary model doesn't fit the data. As such, potential errors from discrepancies between the measured and modeled data attributed to model inadequacies, are reduced between tomographic steps.

Choosing an appropriate secondary model is paramount to be able to differentiate between structured residual from erroneous biological model fitting and residuals originating from random noise. Usually temporal correlation between the residuals signifies potential biological information that cannot be modeled by the primary model. One option then is to use smooth basis function to try and capture this temporal dependency. Another data driven approach, is to decompose the residuals into a number of components and use the  $x$  components with the highest eigenvalues as the secondary model matrix. This approach is based on the fact that kinetics not modeled by the primary model are likely to occur within many image voxels and hence will appear as structure in the covariance matrix of the residuals. The space spanned by each method can be used separately or in combination to create the secondary model.

The algorithm executes as follows:

- i) Start with initial image estimate  $\lambda_{jl}^{(k)}$ .
- ii) Perform one image update over all temporal frames with conventional OSEM to calculate  $\lambda_{jl}^{(k+1)}$ .
- iii) Fit the primary kinetic model in image space using  $\alpha^{(k)}$  as initial estimate to calculate updated parameters  $\alpha^{(k+1)}$ .
- iv) Evaluate the model to calculate fitted image  $f_{jl}(\alpha^{(k+1)})$ .
- v) Calculate primary model residuals  $\lambda_{jl}^{(k+1)} - f_{jl}(\alpha^{(k+1)})$ .
- vi) Project residuals onto secondary model space and calculate the fraction ( $\kappa_j$ ) of the residuals described by the secondary model ( $g_j$ ) to be included back in the image

$$\text{with } \left( \kappa_j = \frac{1}{1+\beta} = \left[ \frac{1-r_{df}}{1-r_{df}+r_{RSS}} \right] \right)$$

- vii) Evaluate adaptive model to calculate new fitted image  $\lambda_{jl}^{(k+1)} = f_{jl}(\alpha^{(k+1)}) + \kappa_j g_j$  and repeat from ii)

where  $j$  and  $l$  refer to the voxel and frame indices,  $\beta$  is a

penalty term trading the primary and secondary models,  $r_{df}$  is the ratio of the degrees of freedom of the secondary model to the remaining degrees of freedom after fitting the primary model, while  $r_{RSS}$  is the proportion of the residual sum of squares described by the secondary model, to the total residual sum of squares after the application of the primary model.

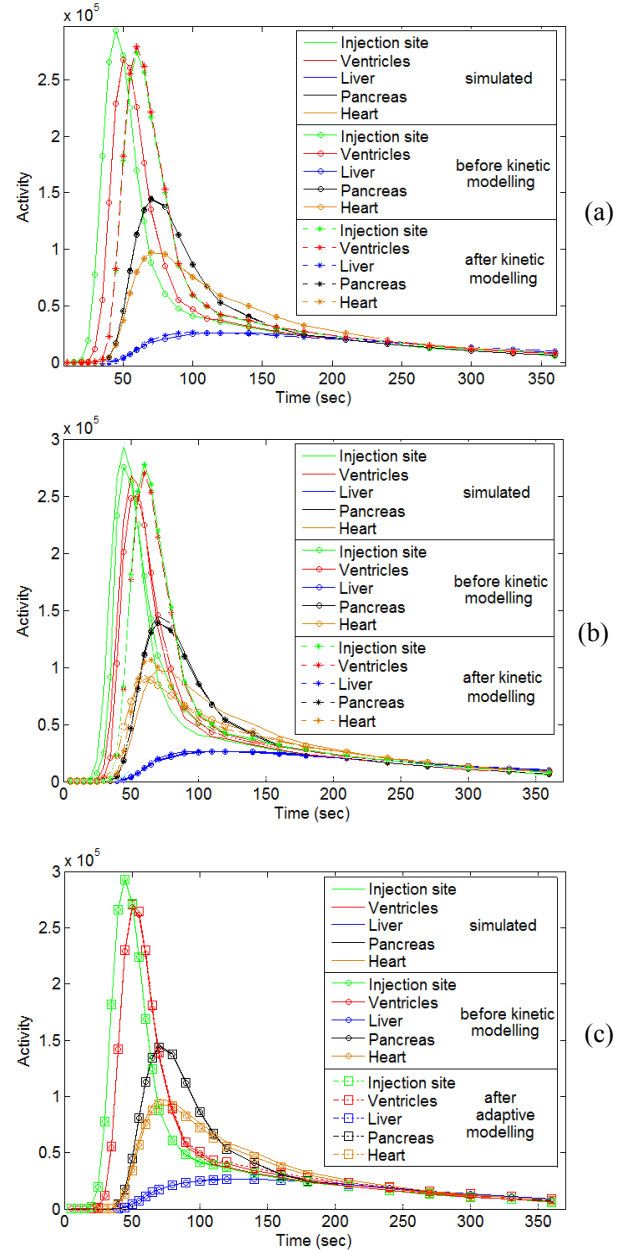


Fig. 1. Simulated time-activity curves (TACs), before and after kinetic modeling, from the complex dataset for the post-reconstruction kinetic analysis (a), the 4-D reconstruction (b) and the adaptive 4-D reconstruction (c) at the 15th iteration (21 subsets). The TACs are shown for badly modeled regions (injection site, ventricles and liver) and 2 well-modeled regions (pancreas and heart). Using the adaptive 4-D method, the TACs from badly modeled regions match the simulated ones after using a secondary model to model the residuals, ensuring a good fit to the data even though the primary model results in a bad fit in these regions.

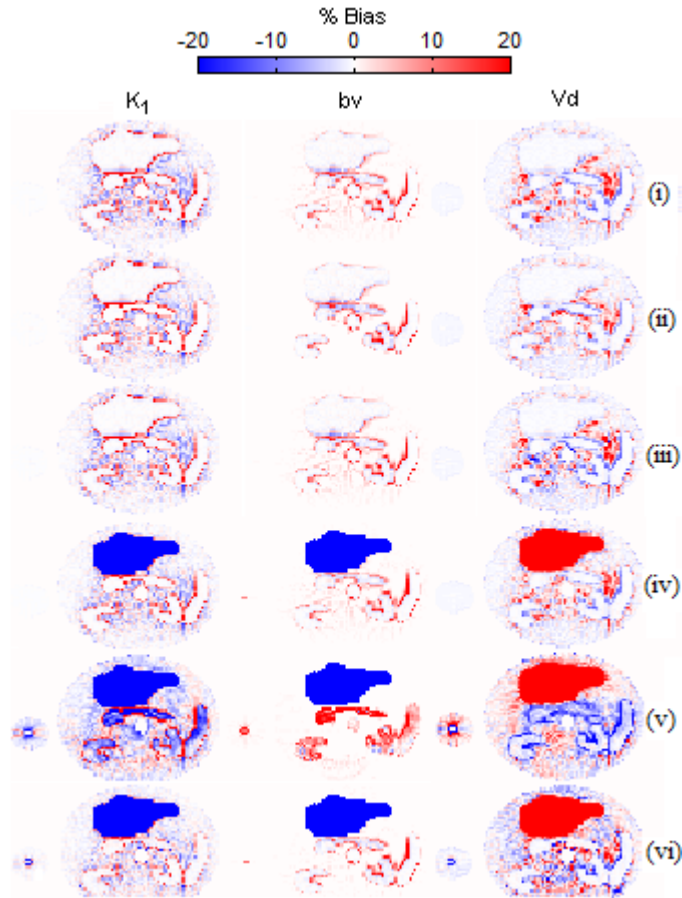


Fig. 2 Parametric images of  $K_1$ , blood volume and  $V_d$  bias for the 1<sup>st</sup> simple (i-iii) and 2<sup>nd</sup> complex noiseless dataset (iv-vi) using post-reconstruction kinetic modeling (i,iv), conventional 4-D image reconstruction (ii, v) and the proposed adaptive 4-D reconstruction (iii, vi). In the adaptive method 4 singular values are used in the secondary model.

### III. METHODS

To evaluate the algorithm, typical [ $^{15}\text{O}$ ]- $\text{H}_2\text{O}$  kinetics were simulated using a 4-D digital phantom with time-activity curves (TACs) representing a 3 parameter 1-tissue model ( $K_1$ ,  $k_2$ , blood volume). Ten regions of interest were used on the phantom representing major internal body structures. Two datasets, one with simple and one with complex and challenging kinetics were generated. In the 1<sup>st</sup> dataset, all regions shared a common input function (IF) using a single input model. In the 2<sup>nd</sup> dataset, an IF with differential delay and dispersion was used to generate the TACs in the heart ventricles and injection site compared to the rest of the regions (no delay and dispersion), while a dual input model was used in the liver (hepatic artery + portal vein) compared to other regions (single input model). The dynamic images from both datasets were forward projected into a virtual scanner with the geometry configuration of the Siemens HiRez PET/CT to create the dynamic projection data. Poisson noise was then introduced and 50 noisy realizations were generated for each dataset.

Both datasets were reconstructed using the adaptive 4D reconstruction, as well as conventional 4D reconstruction without adaptive modeling and 3D reconstruction followed by

kinetic modeling for comparison. For the primary biologic model, we used a 3 parameter, 1-tissue single input model, with no delay and dispersion in the IF. As such the model is representative of all the regions in the 1st simple dataset while in the 2nd dataset is representative of all regions apart from the injection site and heart ventricles due to mismatch in the delay of the input function as well as the liver due to a dual input supply. The generalized linear least square (GLLS) method was used to generate parametric maps. To initialize the kinetic parameters for GLLS, the linear least square (LLS) method was used, which requires no self-initialization. In the adaptive 4D reconstruction, a data driven method was used in order to generate the secondary residual model. The covariance matrix of the residuals was decomposed using singular value decomposition and variable numbers of singular values were used in order to assess the impact of secondary model dimensionality on bias propagation.

### IV. RESULTS

#### A. Impact of adaptive 4-D reconstruction on time-activity curves

Fig. 1 shows the simulated time-activity curves as well as the ones before and after the kinetic modeling step using the post-

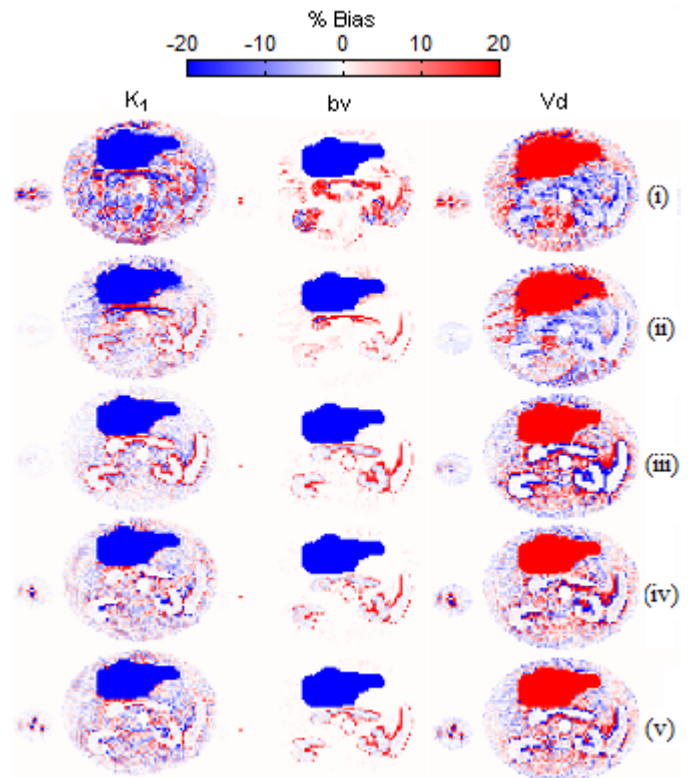


Fig. 3 Parametric images of  $K_1$ , blood volume and  $V_d$  bias for the 2<sup>nd</sup> complex dataset obtained with the proposed adaptive 4-D image reconstruction using an increasing number of singular values (1 SV (i), 2 SV (ii), 3 SV (iii), 5 SV (iv) and 8 SV (v) ) for the secondary model (noiseless data).

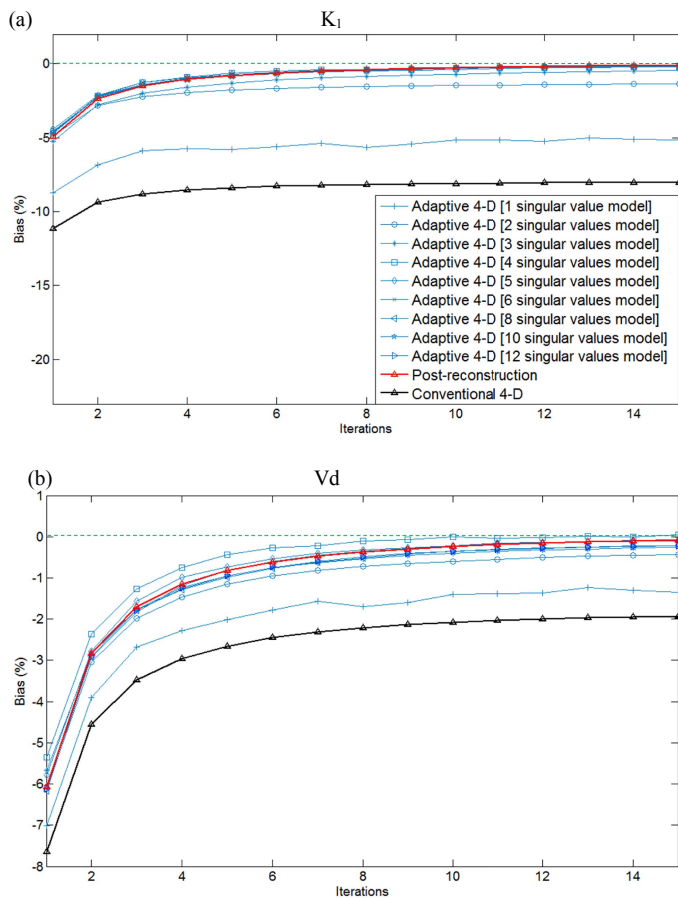


Fig. 4 Bias as a function of iterations for  $K_1$  (a) and  $V_d$  (b) for a region of interest covering the entire pancreas (well-modeled region from the complex dataset) for all the parameter estimation methods (noiseless data). As more singular values are used for the secondary model in the adaptive method bias due to propagation converges to zero, similar to post reconstruction analysis.

reconstruction kinetic analysis (Fig 1(a)), the conventional 4-D reconstruction (Fig 1(b)) and the proposed adaptive 4-D reconstruction, (Fig 1(c)) at the 15<sup>th</sup> tomographic iteration (21 subsets). TACs are taken from the complex dataset and include both badly-modeled (injection site, ventricles and liver) as well as representative well-modeled (pancreas, heart myocardium) regions. Looking at the post-reconstruction analysis, the TACs corresponding to the well modeled regions, before as well as after kinetic modeling coincide with the simulated TACs, as the reconstruction has almost converged and there is a good fit. This is expected since there is a good match between the simulated kinetics and the model used for parameter estimation. In the badly modeled regions however, due to the model used for parameter estimation not being representative of the simulated kinetics, a bad fit is obtained. The TACs in the injection site and ventricles are shifted due to the erroneous delay used, while the liver TAC is biased due to using a single input model as opposed to a dual input model. Moving to the 4-D reconstruction, in badly modeled regions the TACs are biased even before the kinetic modeling step. This is due to the fact that the TACs are shown at the 15<sup>th</sup> iteration and with the 4-D

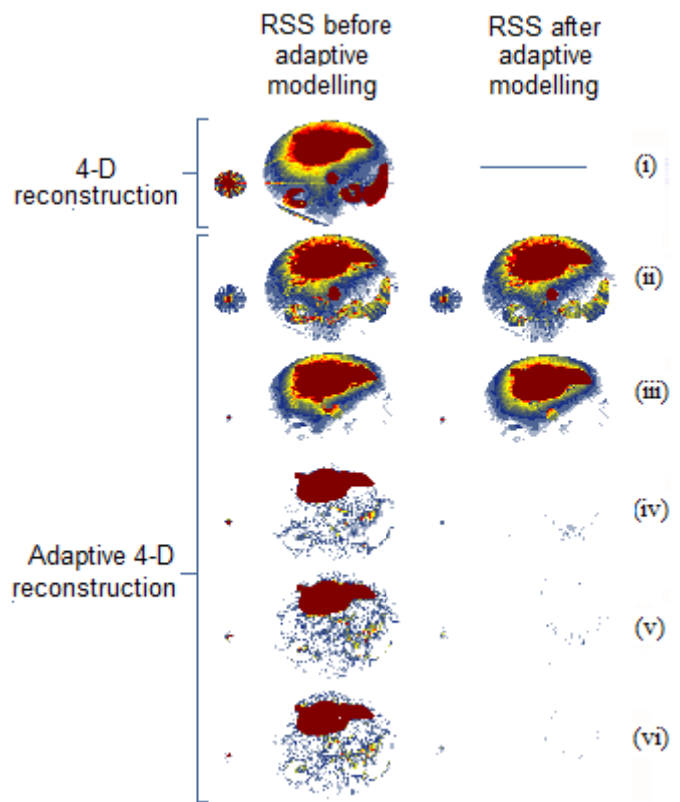


Fig. 5 Parametric images of the residual sum of squares for the complex dataset (noiseless data) before and after adaptive modeling at the 15<sup>th</sup> tomographic iteration using an increasing number of singular values for the secondary model space (1 SV (ii), 2 SV (iii), 3 SV (iv), 5 SV (v) and 8 SV (vi)). The residual sum of squares is also shown for the conventional 4-D reconstruction for comparison.

reconstruction alternating between the tomographic and kinetic modeling steps, the erroneous model has been applied in these regions multiple times. Also looking at the well modeled regions, the TACs before and after the kinetic modeling step no longer coincide with the simulated ones. This is due to bias from badly modeled regions propagating during the previous iterations in these well-modeled regions, creating bias in the parameter and TAC estimates during kinetic modeling. Finally looking at the proposed adaptive method, the TACs in the badly modelled regions coincide with the simulated TACs. As such, using the adaptive modeling, TACs from badly modeled regions are no longer biased after the kinetic modeling step and as a consequence no bias is propagating to well modeled regions during the tomographic step.

#### B. Impact of adaptive 4-D on the spatial propagation of model induced bias - noiseless data

To evaluate the effect of the proposed algorithm on the kinetic parameters, parametric images of bias for 3 parameters and for both simulated datasets are shown in Fig. 2 (15 iterations - 21 subsets). In the 1<sup>st</sup> dataset where there is a good match between the simulated and modeled kinetics, the

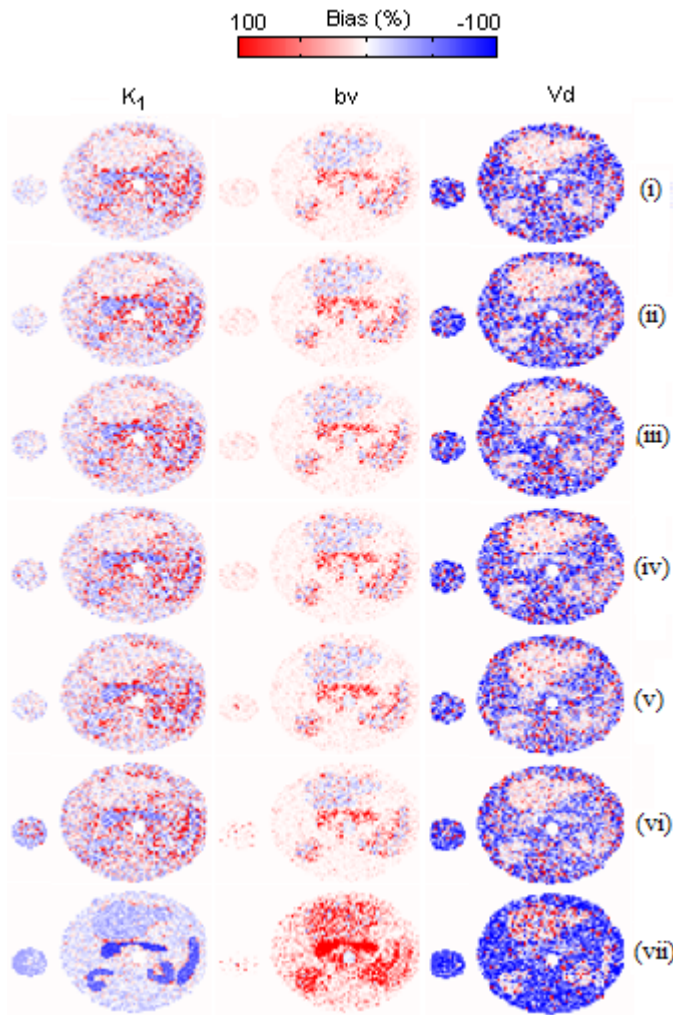


Fig. 6 Parametric images of mean bias over the noisy realizations for the 1<sup>st</sup> simple dataset using conventional 4-D image reconstruction (i), the proposed adaptive 4-D reconstruction with 1 (ii), 2(iii), 3(iv), 5(v) and 8(vi) singular values in the secondary model, as well as the post-reconstruction kinetic modeling (vii).

adaptive 4D reconstruction (Fig. 2 (iii)) delivers parametric maps with almost zero bias in all parameters, similar to the results obtained by the post-reconstruction kinetic analysis (Fig. 1 (i)). As all regions are well modeled in this dataset and no structured residuals exist after the kinetic modeling step, the adaptive 4-D reconstruction behaves similarly to the non-adaptive 4-D reconstruction (Fig. 1 (ii)). When there are complex kinetics in the FOV and there is a discrepancy between the simulated and modeled kinetics (in the injection site, ventricles and liver), the conventional 4D reconstruction (Fig. 1 (v)) delivers biased parametric maps outside of these regions contrary to the post-reconstruction (Fig. 1 (iv)), where errors are localized as was also found in [4]. Using the proposed adaptive 4-D, the bias maps appear to be substantially improved (Fig. 1 (vi)) with the bias in the vicinity of, but outside the liver (spleen, pancreas and kidneys) and injection site almost completely eradicated and resembling the post-reconstruction parametric maps with the bias localised in the liver and injection site (Fig. 1 (iv)).

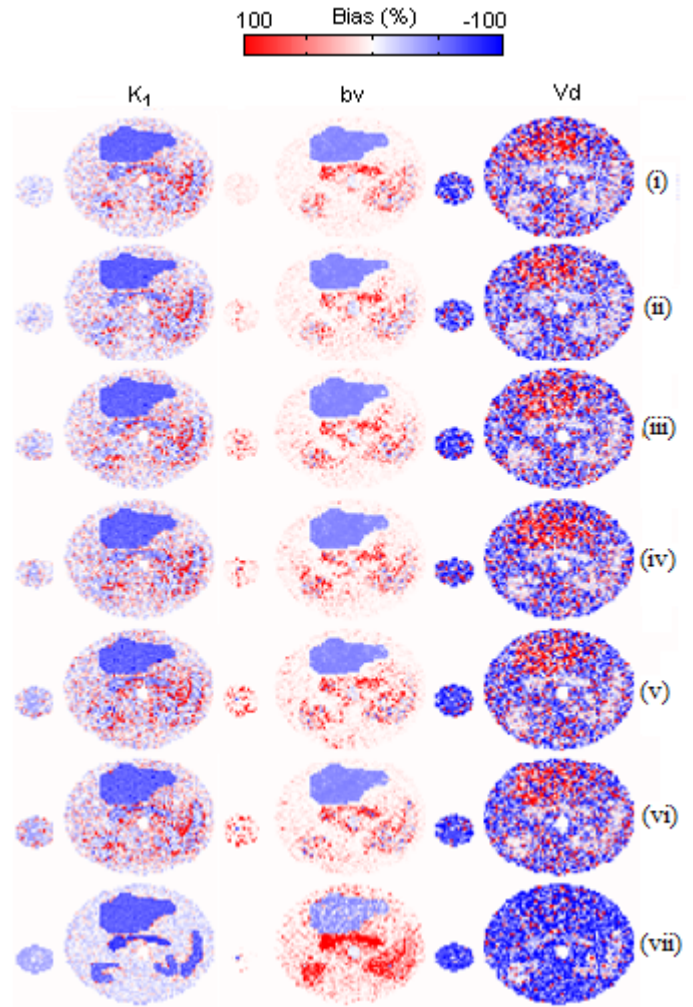


Fig. 7 Parametric images of mean bias over the noisy realizations for the 2<sup>nd</sup> complex dataset using conventional 4-D image reconstruction (i), the proposed adaptive 4-D reconstruction with 1 (ii), 2(iii), 3(iv), 5(v) and 8(vi) singular values in the secondary model, as well as the post-reconstruction kinetic modeling (vii).

### C. Impact of secondary model on residuals and spatial propagation of model induced bias - noiseless data

One parameter that is crucial in trying to identify and model structured residuals as opposed to noise is the choice of the secondary model and its dimensionality. In Fig. 3 parametric images of bias are shown for  $K_1$ , blood volume and  $V_d$  for the complex dataset, where there are structured residuals, using an increasing number of singular values as a secondary model space. Using only the first singular value no improvement is seen in the parameters, with bias propagation still affecting the well-modeled regions. When 2 singular values are used, bias propagation is substantially reduced with bias only localized in the badly modeled regions, while further improvements are obtained when using 3 or more singular values. This is due to the fact that as more singular values are included in the secondary model, more of the structured residuals are modeled by the secondary model. Quantitative evaluation is shown in Fig.4 where  $K_1$  (Fig. 4(a)) and  $V_d$  (Fig. 4(b)) bias is plotted as

a function of iterations for all reconstruction methods, for a region of interest in the pancreas (well-modeled region) from the complex dataset. Negative bias is seen in both  $K_1$  and  $V_d$  in the conventional 4-D reconstruction due to propagation from badly modeled regions. Using the adaptive 4-D method, the bias due to propagation is progressively reduced as more singular values are included in the secondary model, approaching the zero bias seen in the post-reconstruction analysis. This trend is reflected in Fig 5 where the residual sum of squares (RSS) corresponding to the parametric images of Fig. 3 are shown, before the adaptive modeling (after fitting the primary model) and after the adaptive modeling (after using the secondary model and putting a portion of the residuals back into the dynamic image sequence) at the 15<sup>th</sup> iteration. When the first 2 singular values are used for the secondary model (Fig. 5 (ii,iii)), only a small portion of the structured residuals is modeled, with the RSS being similar before and after the adaptive modeling. As more singular values are used, structured residuals are only visible in the badly modeled regions before the application of the adaptive

modeling, with the well modeled regions having no residuals due to propagation. This is due to the fact that even though the RSS is shown before the adaptive modeling for that tomographic iteration, the adaptive modeling has been applied multiple times during the previous iterations. After the adaptive modeling no structured residuals exist both in the well and badly-modeled regions meaning that a good fit is obtained in all image voxels.

#### D. Impact of adaptive 4-D reconstruction on noise induced bias and the spatial propagation of model induced bias - noisy dataset

Under noisy conditions the behaviour of the different algorithms becomes even more complex. Fig. 6 shows parametric images of mean bias over 50 noisy realizations for  $K_1$ , blood volume and  $V_d$  for the simple dataset, estimated using the conventional 4-D reconstruction (Fig. 6(i)), the post-reconstruction kinetic analysis (Fig. 6 (vii)) and the adaptive 4-D reconstruction using a variable number of singular values in the secondary residual model (Fig. 6 (ii-vi)). As already seen in [4] the conventional direct 4-D method delivers substantial improvements in bias compared to the post-reconstruction analysis. Using the adaptive 4-D in this dataset, where there are no structured residuals due to erroneous model formulation, and progressively increasing the dimensionality of the secondary model, results in gradually modeling unstructured noise in the residuals. Putting back into the dynamic image sequence residuals due to noise, gradually increases bias in the kinetic parameter. However even when 8 singular values are used in the adaptive method, the bias in the parameters is still substantially lower compared to the post-reconstruction method and only slightly increased compared to the conventional 4-D method.

Moving to the complex dataset where there are structured residuals Fig. 7 again shows parametric images of mean bias over 50 noisy realizations for  $K_1$ , blood volume and  $V_d$  estimated using the conventional 4-D reconstruction (Fig. 7(i)), the post-reconstruction kinetic analysis (Fig. 7 (vii)) and the adaptive 4-D reconstruction using a variable number of singular values in the secondary residual model (Fig. 7 (ii-vi)). As observed in [4], even though the conventional 4-D reconstruction has reduced noise-induced bias compared to the post-reconstruction analysis in well modeled regions, these suffer from additional bias spatially propagating from badly modeled regions, reducing the benefits of the direct 4-D method. Using the adaptive method, initially, a similar trend is seen as in Fig. 6, with randomly distributed bias in the kinetic parameters increasing when increasing number of singular values are used. Also based on Fig. 3 one would expect bias due to propagation to start decreasing as more singular values are used. As such comparing the bias in a well modeled region from the simple dataset in Fig. 6 (noise induced bias) with the bias in the same region from the complex dataset in Fig. 7 (noise induced bias + bias due to propagation) can reveal any bias propagation reduction. However it is very difficult to visually compare bias between the 2 datasets as the magnitude of the bias due to propagation is substantially lower compared to the noise induced bias and quantitative analysis is needed.

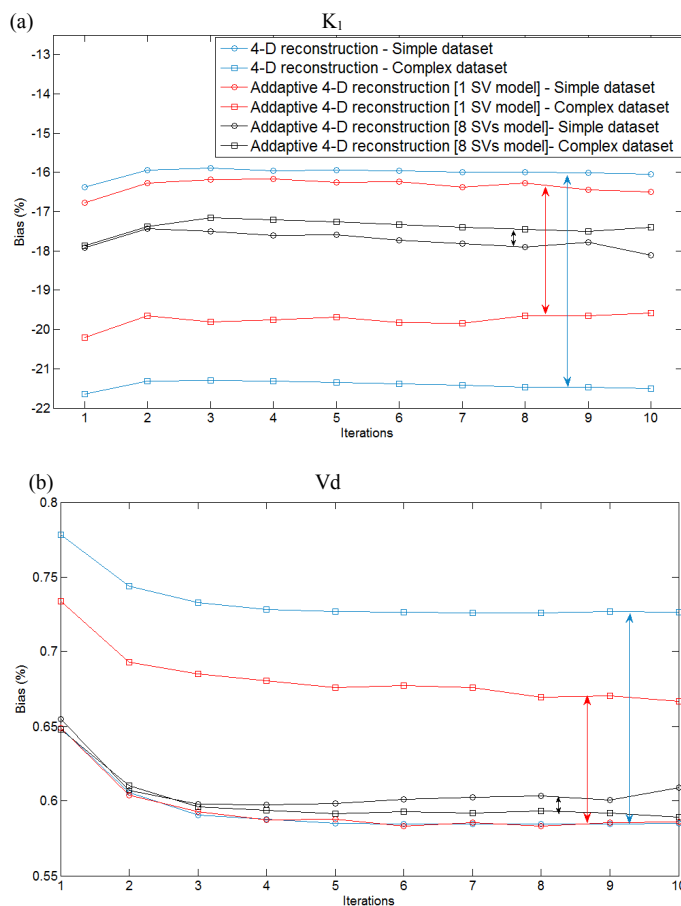


Fig. 8. Bias as a function of iterations for  $K_1$  (a) and  $V_d$  (b) for a region of interest covering the entire pancreas (well-modeled region) for both datasets and using the conventional 4-D reconstruction as well as the adaptive 4-D reconstruction with 1 and 8 singular values in the secondary model. As more singular values are used for the secondary model in the adaptive method bias due to propagation converges to zero, similar to post reconstruction analysis.

In Fig. 8  $K_1$  and  $V_d$  bias for a well-modeled region (pancreas) is plotted for the simple and the complex datasets, using the adaptive 4-D method with 1 and 8 singular values representing the extreme cases, as well as using the conventional 4-D method for comparison. Using the conventional 4-D reconstruction the bias level seen in the simple dataset is due to noise with the additional bias in the complex dataset due to bias propagation. When the adaptive methods is used with 1 singular value, the noise induce bias in the simple dataset is slightly increased compared to the conventional 4-D, but at the same time the additional bias due to propagation has now been reduced, looking at difference to the complex dataset. Using 8 singular values again a further slight deterioration is seen in the noise induced bias, looking at the simple dataset, due to modeling unstructured residuals from noise. However, bias in the complex dataset almost coincides with that from the simple dataset, signifying that bias due propagation has substantially been reduced. Similar trends are seen both in  $K_1$  and  $V_d$ .

- [2] Wang and Qi, IEEE Trans. Med. Imaging, 2009, **28**(11), pp 1717-1726
- [3] J. Yan et al, IEEE NSS-MIC Conf. Rec. 2010, M09-261
- [4] F. Kotasidis et al. IEEE NSS-MIC Conf. Rec, 2011, pp 2366-2367
- [5] J. Matthews et al IEEE NSS-MIC Conf. Rec, 2012 , M22-36

## V. DISCUSSION & CONCLUSION

A new approach to direct parametric reconstruction is implemented and evaluated. The method uses a new kinetic modeling strategy based on the adaptive inclusion of structured residuals due to erroneous model formulation, back into the image. However it has to be emphasized that the adaptive method doesn't affect the kinetic parameters in those erroneously modeled regions estimated during the primary model fit, but only improves the data fit. It is this improved fit in the badly modeled regions in the kinetic model step that can prevent bias propagating in the well modeled regions during the tomographic step, indirectly improving parameter bias in these regions and helping 4-D reconstruction deliver its full potential.

Results based on noiseless and noisy datasets, demonstrate that kinetic model induced bias propagation in kinetic parameters is significantly suppressed using the proposed 4-D image reconstruction method. The observed improvements, however, greatly depend on the secondary model. Under noisy conditions this model selection becomes even more crucial as using inappropriate models which are too unconstrained, result in the inclusion of unstructured residuals due to noise back into the image, reducing the benefits of 4-D image reconstruction. As such, bias improvements in the parameters due to reduced error propagation are obtained at the expense of a small increase in noise induced bias, with the overall bias though reduced compared to the traditional 4-D reconstruction.

## ACKNOWLEDGEMENTS

This work was supported by the Swiss National Science Foundation under grant SNSF 31003A-135576,

## REFERENCES

- [1] J. Matthews et al, IEEE NSS-MIC Conf. Rec, 2010, pp 2435 - 2441